K. RZYMAN[*]   J.-C. GACHON [**][1]

FORMATION ENTHALPY OF AlNi₃-BASED ALLOYS WITH IRON ADDITIONS BY CALORIMETRIC SOLUTION AND DIRECT REACTION METHODS

ENTALPIA TWORZENIA STOPÓW NA OSNOWIE AlNi₃ Z UDZIAŁEM ŻELAZA WYZNACZONA KALORYMETRYCZNĄ METODĄ ROZPUSZCZANIA ORAZ METODĄ BEZPOŚREDNIEJ REAKCJI

The enthalpies of formation of AlNi₃-based alloys with iron additions were determined both by solution and direct reaction calorimetry. The results were analyzed in order to determine phase boundaries in the pseudo-binary AlNi₃-FeNi₃ system.

Keywords: AlNi₃, calorimetry, formation enthalpy, solution method, direct reaction method

Entalpia tworzenia stopów na osnowie AlNi₃ z udziałem żelaza została wyznaczona doświadczalnie kalorymetryczną metodą rozpuszczania oraz metodą bezpośredniej reakcji. Uzyskane wyniki przeanalizowano pod kątem wyznaczenia granic międzyfazowych w badanym pseudo-binarnym układzie AlNi₃-FeNi₃.

1. Introduction

The intermetallic compound AlNi₃ ($L1_2$, fcc), belongs to the group of materials frequently placed between metals and ceramics. Properties of AlNi₃-based alloys make them high temperature construction material candidates. They are superior to classic creep-resisting Ni-based superalloys. Their advantages are: higher strength parameters at elevated temperatures, increasing yield point with increasing temperature, higher fatigue resistance, higher creep strength, very good resistance to grinding and erosion wear, high resistance to oxidation, also at high temperature [1].

The disadvantage of AlNi₃ is its brittleness. The introduction of some additions accounts for promising results in increasing ductility. Iron, which belongs to this group [2÷5], exhibits a considerable range of solubility, 14 at.% Fe, in AlNi₃-based γ' ordered phase [6]. Iron substitutes both Ni and Al on their sites [7÷9]. The above is reflected in the direction of the solubility lobe [6] which aims at ca. $Fe_{55}Ni_{45}$ composition on the Ni-Fe boundary.

The paper presents the study on formation enthalpies of $Ni_{75}Al_{25-X}Fe_X$ alloys. The alloy compositions were chosen due to their predicted application. According to literature data [10,11], pseudobinary alloys in the range AlNi₃-FeNi₃ have a considerable potential for industrial application. Accurately determined thermodynamic properties give way to precise determination of phase equilibria, the knowledge of which helps obtaining the optimal microstructure of ordered γ' and disordered γ domains in suitable proportions.

2. Experimental

Formation enthalpies of AlNi₃-based alloys with iron additions were determined experimentally by two independent calorimetric techniques: solution and direct reaction methods.

2.1. Solution method

This method is based on comparison of dissolution heat of the alloy and its components in a solvent, here liquid Al. The enthalpies of formation $\Delta_f H$ of $Ni_{75}Al_{25-x}Fe_x$ alloys were determined with the following equation:

[*] SILESIAN UNIVERSITY OF TECHNOLOGY, FACULTY OF MATERIALS ENGINEERING AND METALURGY, DEPARTMENT OF METALLURGY , 40-019 KATOWICE, KRASINSKIEGO STREET 8, POLAND

[**] RETIRED, FORMERLY WITH THE LCSM, UMR7555, NOW A PART OF IJL, UMR 7198, FRANCE

$$\Delta_f H_{Ni75Al(25-x)Fex} = 0.75\Delta H_{Ni}^{ef} + 0.01(25-x)\Delta H_{Al}^{ef} + \\ +0.01x\Delta H_{Fe}^{ef} - \Delta H_{Ni75Al(25-x)Fex}^{ef} \tag{1}$$

where:

75, (25-x), x – atomic percentage of Ni, Al, Fe, respectively

0.75, 0.01(25-x), 0.01x – mole fraction of Ni, Al, Fe respectively

ΔH_{Ni}^{ef}, ΔH_{Al}^{ef}, ΔH_{Fe}^{ef}, $\Delta H_{Ni75Al(25-x)Fex}^{ef}$ – heat effects accompanying dissolution of the components and the alloy in the bath.

Special container was installed in the calorimeter which made it possible to anneal the samples at 1123K before dropping them into the bath. Thus enthalpies of formation were determined at 1123K.

For determination of ΔH_{Ni}^{ef}, ΔH_{Al}^{ef}, ΔH_{Fe}^{ef}, our own data for H_{Ni}^0, H_{Fe}^0 [12] (partial heat of solution in liquid aluminum of Ni and Fe at infinite dilution, respectively) and thermochemical data from [13] were applied. $\Delta H_{Ni75Al(25-x)Fex}^{ef}$ values were experimentally determined.

Partial enthalpies of dissolution for Ni and Fe at 1123K were $H_{Ni}^0 = -149.2 \pm 0.6$ kJ/mole of atoms, $H_{Fe}^0 = -120.6 \pm 1.1$ kJ/mole of atoms [12].

Samples were annealed at 1123K outside the calorimeter in argon for 150 hours and rapidly quenched. Then they were annealed for 4 hours at 1123K inside the calorimeter in the intermediate container just before dropping them into the bath.

Calibration was performed prior to measurements by dropping aluminum samples into the bath. Application of aluminum, which was one of the alloys components as the material for calibration, helped avoid one experimental series and reduce the experimental error.

The reference state was solid for both components and alloys.

2.2. Direct reaction method

The measurements of heat effects accompanying direct reaction of powder components at elevated temperature in the calorimeter were the basis for determination of formation enthalpies.

Calibration and reaction samples were dropped from room temperature to the elevated temperature of the reaction crucible. The synthesis of studied $Ni_{75}Al_{(25-x)}Fe_x$ alloy can be presented by the following equation:

$$0.75Ni(\text{room temp.}) + 0.01(25-x)Al(\text{room temp}) + \\ +0.01xFe(\text{room temp}) = \\ Ni_{75}Al_{(25-x)}Fe_x(\text{calor.temp.}) + Q \tag{2}$$
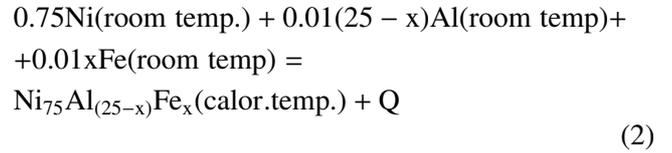
The total amount of heat (Q) is the algebraic sum of formation enthalpy

$\Delta_f H_{Ni75Al(25-x)Fex}$ and heat contents $0.75\Delta H_{room}^{calor}(Ni)$, $0.01(25-x)\Delta H_{room}^{calor}(Al)$, $0.01x\Delta H_{room}^{calor}(Fe)$ of components from room temperature to the temperature of the reaction crucible. The data from [13] were used for calculations of component heat contents. The enthalpy of formation can be calculated from the equation:

$$\Delta_f H_{Ni75Al(25-x)Fex} = Q - [0.75\Delta H_{room}^{calor}(Ni) + \\ +0.01(25-x)\Delta H_{room}^{calor}(Al) + 0.01x\Delta H_{room}^{calor}(Fe)] \tag{3}$$

Samples used for calibration (α-Al_2O_3) and samples for measurements of enthalpies of formation (pressed mixture of components) were placed alternately in a special dispenser kept under argon which was installed on the top of the calorimeter.

As well as in the solution method the solid state of substances was chosen as a reference state.

Details of both solution and direct reaction calorimeters as well as experimental procedures have been previously described in this periodical [14].

3. Results

The results obtained by calorimetric solution and direct reaction methods are presented in Table 1 and 2, respectively. The results obtained by both methods are also presented in Fig. 1.

Results obtained by calorimetric solution method for $Ni_{75}Al_{25-x}Fe_x$ alloys; samples were dropped into the bath from 1123K;
temperature of the bath = 1123K

Iron content [at.%]	Sample no.	Heat effects accompanying dissolution of $Ni_{75}Al_{25-x}Fe_x$ alloy in liquid aluminum [kJ/mole of atoms]
0	1	-57.7
	2	-57.3
	3	-56.8
	4	-58.6
	5	-57.6
	6	-56.0
	7	-59.2
	Average value: -57.6±1.1	
	Formation enthalpy = -42.3±1.6 kJ/mole of atoms	
2	1	-40.7
	2	-40.9
	3	-42.9
	4	-42.6
	Average value: -41.8±1.1	
	Formation enthalpy = -41.8±1.6 kJ/mole of atoms	
4	1	-63.0
	2	-65.4
	3	-64.0
	4	-63.4
	5	-65.3
	Average value: -64.2±1.1	
	Formation enthalpy = -40.4±1.5 kJ/mole of atoms	
6	1	-68.1
	2	-69.6
	3	-71.4
	Average value: -69.7±1.7	
	Formation enthalpy = -37.1±2.2 kJ/mole of atoms	
8.5	1	-81.0
	2	-85.4
	3	-82.0
	4	-84.3
	Average value: -83.2±2.0	
	Formation enthalpy = -26.6±2.5 kJ/mole of atoms	
11	1	-94.2
	2	-91.8
	3	-91.6
	4	-89.5
	5	-95.0
	6	-93.1
	Average value: -92.5±2.0	
	Formation enthalpy = -20.3±2.5 kJ/mole of atoms	

Formation enthalpy of $Ni_{75}Al_{25-x}Fe_x$ alloys determined by the method of direct synthesis; room temperature = 300K; temperature of the reaction crucible = 1132K

Iron concentration [at.%]	Formation enthalpy [kJ/mole of atoms]
0	-39.4
	-39.1
	-39.0
	-39.8
	Average value = -39.4±0.6
2	-40.4
	-38.0
	-40.7
	-39.2
	-40.1
	Average value = -39.7±1.1
4	-37.7
	-38.2
	-38.3
	-36.7
	-39.5
	Average value = -38.1±1.1
6.5	-34.3
	-33.7
	-34.4
	-34.6
	-33.9
	Average value = -34.2±0.6
9	-28.4
	-28.6
	-29.4
	-28.9
	-28.6
	Average value = -28.8±0.6
12	-23.3
	-23.4
	-23.7
	-22.7
	-23.4
	Average value = -23.3±0.6
15	-16.0
	-17.0
	-18.2
	Average value = -17.1±1.2

TABLE 2 cd

1	2
	-11.6
	-12.8
	-13.2
18	-13.1
	Average value = -12.7±0.8
	-9.1
21.5	-7.1
	Average value = -8.1±1.5
	-4.5
	-4.8
	-3.8
	-3.9
25	-3.9
	Average value = -4.2±0.6
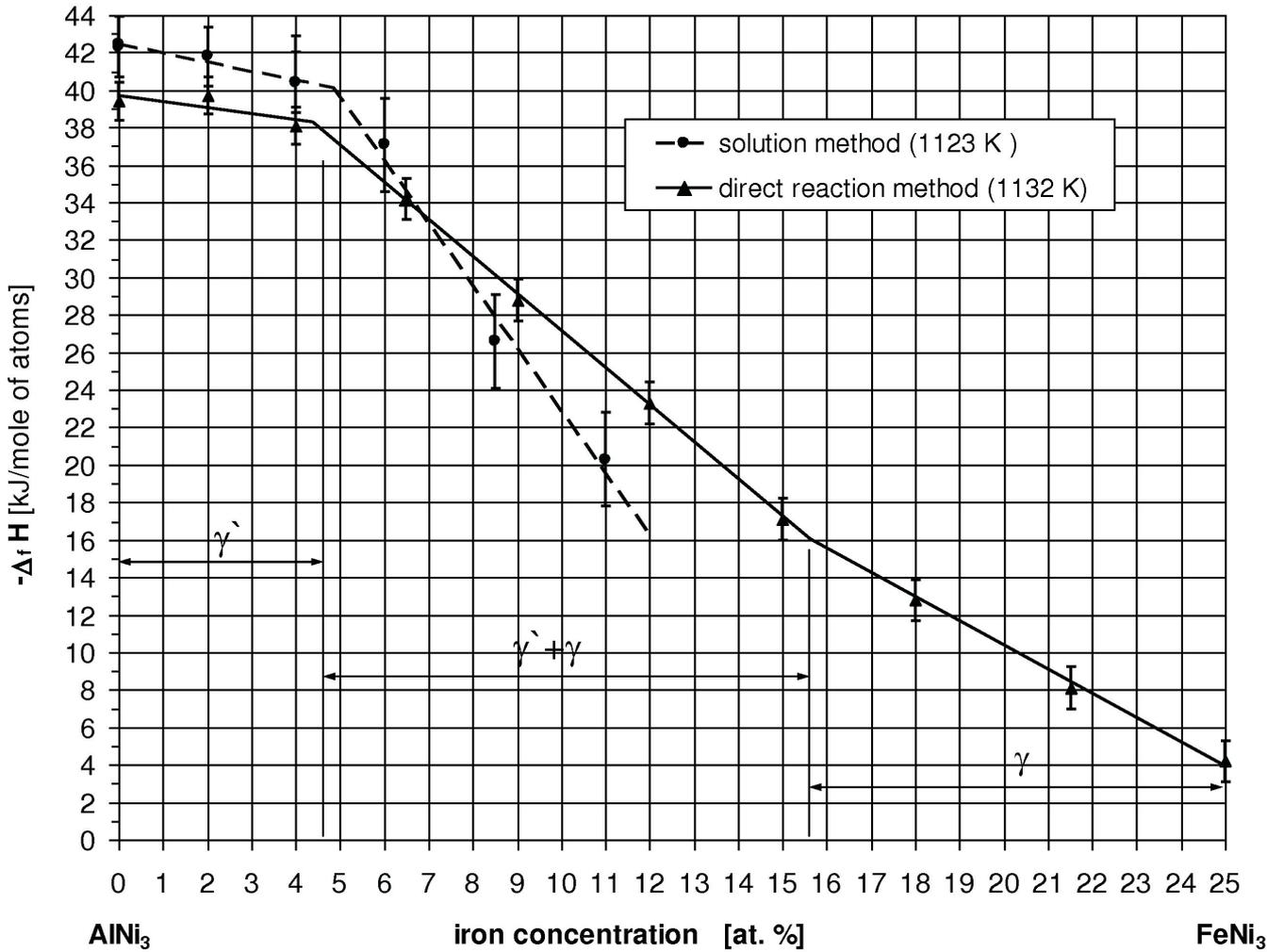
Fig. 1. Formation enthalpy of $Ni_{75}Al_{25-x}Fe_x$ alloys obtained by calorimetric solution and direct reaction method

4. Disscusion

Negative values of formation enthalpy of $Ni_{75}Al_{25-x}Fe_x$ alloys varying in a wide range from $-42 \div -4$ kJ/mole of atoms were obtained. The highest negative value of formation enthalpy was noted for $AlNi_3$ – it equals -42.3 ± 1.6 and -39.4 ± 0.6 kJ/mol of atoms obtained by us by solution [15] and direct reaction [12] methods, respectively. It is understandable because the intermetallic compound $AlNi_3$ crystallizes in high-ordered structure $L1_2$ with high density packing of atoms which is accompanied by a strong bonding between them. Ellner [16] noted 8% reduction of aluminum atom radius in $AlNi_3$ as compared with atom radius in pure metal which also proves the tightly spacing of atoms in $AlNi_3$. Schubert [17] proved that the arrangement of atoms in $AlNi_3$ is particularly convenient from the energy view point and is reflected in high negative formation enthalpy presented in this paper. High ordering in $AlNi_3$ is reflected in high negative excess entropy value. Integral excess entropy of formation ΔS^{ex} = -12.9 J/K mol of atoms at 1045K was obtained with the use of excess integral free enthalpy values from electrochemical studies [18] and of $\Delta_f H$ from [15].

In general, the addition of iron reduces the absolute value of formation enthalpy of $Ni_{75}Al_{25-x}Fe_x$ alloys, which is reflected in the results obtained by both calorimetric methods applied.

A distinct break of formation enthalpy dependence is visible at ca. 5 at.%Fe content (solution method) and ca. 4.5 at.%Fe content (direct synthesis).

The results obtained in direct reaction method, where the experiments were performed in the whole range of $AlNi_3 \div FeNi_3$ pseudobinary, exhibit also a second break of $\Delta_f H$ dependence at ca.16 at.%Fe concentration.

Therefore the dependence of formation enthalpy vs. iron content was analyzed dividing it into 2 or 3 segments.

The method of segment approximation, with two segments, was applied for data obtained by solution calorimetry:

$\Delta_f H = A_1 \times at.\%Fe + B_1$ for   at.%Fe<F and
$\Delta_f H = A_2 \times at.\%Fe + B_2$ for   at.%Fe⩾F

or for three segments model (for data from direct reaction method):

$\Delta_f H = A_1 \times at.\%Fe + B_1$ for   at.%Fe<F_1
$\Delta_f H = A_2 \times at.\%Fe + B_2$ for F_1⩽at.%Fe<F_2
$\Delta_f H = A_3 \times at.\%Fe + B_3$ for   at.%Fe⩾F_2

Based on the minimization of mean square deviations, the model parameters were determined estimating the position of boundary points. For boundary values of respective segments the analysis of linear regression was performed. As the results, angular coefficients and constants of linear regression and their statistical significance were obtained. The intersection points of the regression lines were used for accurate boundary determination. The test of parallelism (or equality of regression coefficients) of neighboring segments was carried out. The statistical significance of regression coefficients was determined and allowed to find the presence or absence of parallelism of neighboring segments. It was the basis for justifying the split of formation enthalpy ranges.

It is expressed by the probability (p) of committing the statement error which indicates that the directional coefficients are different. This constitutes the base for dividing the formation enthalpy dependence into segments. Parallelism statistical test proved considerable difference of slopes between the approximated straight lines. The break of formation enthalpy dependence was determined for 4.9 at.%Fe (when $\Delta_f H$ = -40.13 kJ/mol of atoms) with p<0.0001 for the results of solution method. Two breaks were found for the results of direct reaction method: at 4.4 at.%Fe (when $\Delta_f H$ = -38.3 kJ/mol of atoms) with p<0.0001 and at 15.6 at.%Fe (when $\Delta_f H$ = -16.0 kJ/mol of atoms) with p<0.0001.

The determined ranges of formation enthalpy can be attributed to the ranges of occurrence of the respective phases.

Alloys with low iron content (0⩽at%Fe<4.9 – solution method and 0<at%Fe<4.4 – direct reaction method) should be attributed to the ordered γ' phase.

With the increased iron content, the disordered γ phase appears in addition to the ordered γ' phase.

The disordered phase is less energetically bonded than the ordered phase. In case of calorimetric solution method this is shown by lower energy input necessary for bond breaking in dissolution process of the alloy.

In case of direct reaction method it corresponds to lower enthalpy release during the disordered phase formation.

Lower formation enthalpy absolute value is the result in case of both methods.

From 4.9 at.%Fe (solution method) or 4.4 at.%Fe (direct reaction method) we note a considerable decrease of $\Delta_f H$ absolute value with the increase of iron content. The formation enthalpy break with Fe content variation should be attributed to the $\gamma'/\gamma' + \gamma$ phase boundary. In experiments conducted by direct reaction another break was also found at 15.6 at.% of iron. This point can be attributed to the $\gamma' + \gamma/\gamma$ boundary. Alloys with higher iron contents contain γ disordered phase.

The results presented in this paper are generally in accordance with the results of [19], where diffusion couples, X-ray studies, metallography observations were performed, and [20], where diffusion couples method was

used. They are in agreement both with the data determined in [22] (results referred in [23]), where metallography observations, electron probe analysis, differential scanning calorimetry, electrical resistivity studies were performed and with the data in [23] where energy dispersion spectroscopy, EPMA, electrical resistivity, TEM and TEM-EDX studies were carried out. They also agree with the results of [24] where optical observations were carried out.

Phase boundaries obtained in this paper and in [19÷20], [22÷24] are presented in Table 3.

TABLE 3

Phase boundaries $\gamma'/\gamma' + \gamma$ and $\gamma' + \gamma/\gamma$ of AlNi$_3$÷FeNi$_3$ pseudobinary determined in this paper and by other authors. Temperature =1123K, only for direct reaction method T =1132K

Iron content [at%Fe]	Method	Reference position	Remarks
$\gamma'/\gamma' + \gamma$ **phase boundary**			
4.9	Calorimetric solution method	This paper	
4.4	Calorimetric direct reaction method	This paper	
4.8	Diffusion couple method, metallography observations, X-ray diffraction measurements, lattice parameter measurements	[19]	Results mostly extrapolated from higher temperatures
5.6	Diffusion couple method	[20]	Results obtained with use of direct results from table 1 in [20] and extrapolated to 1123K.
4.5	Metallography observations, electron probe analysis, differential scanning calorimetry, electrical resistivity studies	[22]	Results from [22] referred in [23] (fig.5)
5.1	Microscopic investigations	[24]	
$\gamma' + \gamma/\gamma$ **phase boundary**			
15.6	Calorimetric direct reaction method	This paper	
15.2	Diffusion couple method, metallography observations, diffraction measurements.	[19]	Results extrapolated from higher temperature
16.0	Diffusion couple method	[20]	Results obtained with use of direct results from table 1 in [20] and extrapolated to 1123K; T$_{order-disorder}$ of FeNi$_3$ [21] was also taken into account
16.0	metallography observations, electron probe analysis, differential scanning calorimetry, electrical resistivity studies	[22]	Results referred in [23] Results extrapolated from higher temperature
16.0	energy dispersion spectroscopy, EPMA, electrical resistivity, TEM, TEM-EDX studies	[23]	Result based mainly on electrical resistivity measurements
16.3	Microscopic investigations	[24]	

It is worth mentioning that the formation enthalpies given in this paper are valuable because they can be used for determination of phase equilibria in two ways. The first possibility is the determination of phase boundaries as presented in this publication. The second is their use in the CALPHAD procedure.

5. Summary

1. Formation enthalpies of Ni$_{75}$Al$_{25-x}$Fe$_x$ alloys were determined by two calorimetric methods: solution and direct reaction (in case of the latter mathod in the whole range of pseudobinary).

2. Negative values of $\Delta_f H$ varying in a wide range $-42.3 \div -4.2$ kJ/mol of atoms were obtained.

3. The highest negative values of $\Delta_f H$ were obtained for pure $AlNi_3$ (-42.3 ± 1.6 kJ/mol of atoms by solution method and -39.4 ± 0.6 kJ/mol of atoms by direct reaction method). It reflects strong bonding in $AlNi_3$, which crystallizes in ordered $L1_2$ structure (ordered γ' phase). Calculated excess integral entropy takes considerably negative value $= -12.9$ J/K mol of atoms which reflects high-ordered $L1_2$ structure.

4. Addition of iron lowers the absolute values of formation enthalpy. Statistical analysis allowed to determine the break on $\Delta_f H$ dependence for alloy of 4.9 at.%Fe by solution method and 4.4 at.%Fe by direct reaction method. For alloys of higher iron content significant decrease of absolute values of formation enthalpy is noted.

5. For the significant decrease of absolute values of formation enthalpy for alloys with Fe content higher than iron content corresponding to the break on $\Delta_f H$ dependence, the appearance of disordered γ phase is responsible. Disordered γ phase is a phase of higher energy than ordered γ' which is in accordance with ascertained considerable decrease of formation enthalpy. The break of $\Delta_f H$ dependence is attributed to the $\gamma'/\gamma' + \gamma$ phase boundary.

6. The results of formation enthalpy studies by direct reaction method, where experiments were performed in the whole range of $AlNi_3 \div FeNi_3$ pseudobinary, showed another break at 15.6 at.% Fe content. This break is attributed to $\gamma' + \gamma/\gamma$ phase boundary.

7. Satisfactory agreement was found between phase boundaries determined in this paper and the results obtained by other authors.

8. The obtained formation enthalpy data can be used for determination of phase equilibria in two ways. The first is the determination of phase boundaries as it is presented in this publication, availing the breaks on formation enthalpy dependence. The second is the application of formation enthalpies as important values together with other data for determination of phase equilibria with the use of e.g. CALPHAD procedure.

REFERENCES

[1] „Materiały metalowe z udziałem faz międzymetalicznych" ("Metallic materials with intermetallic phases"), edited by Z. Bojar and W. Przetakiewicz, Warszawa, (2006).

[2] T. Takasugi, O. Ozumi and N. Masahashi, Acta Metallurgica 33, 1259 (1985).

[3] A. Inoue, T. Masumoto, Journal of Materials Science 19, 3097 (1984).

[4] C.H. Tsau, J.S.C. Jang, J.W. Yeh, Materials Science and Engineering A152, 264 (1992).

[5] C.T. Liu, Material Research Society Symposium Proceedings 288, 355-367 (1987).

[6] R.W. Guard, J.H. Westbrook, Transactions of Metallurgical Society AIME 215, 807 (1959).

[7] J.R. Nichols and R.D. Rawlings, Acta Metallurgica 25, 187, (1977).

[8] M.K. Miller, J.A. Horton, Scripta Metallurgica 20, 1125 (1986).

[9] S. Pascarelli, F. Boscherini, K. Ławniczak-Jabłońska and R. Kozubski, Physical Review B49, 149 (1994).

[10] B. Giesecke, V.K. Sikka, Materials Science and Engineering A153, 520 (1959).

[11] V.K. Sikka, J.T. Mavity, K. Anderson, Materials Science and Engineering A153, 712 (1992).

[12] K. Rzyman, Habilitation work, "Energy effect accompanying the formation of intermetallic phases", Kraków, 1-110 (2002).

[13] SGTE Substance Data Base, Royal Institute of Technology, Sweden (1994).

[14] K. Rzyman, Z. Moser, J.-C. Gachon, Archives of Metallurgy and Materials 49, (3), 545-563 (2004).

[15] K. Rzyman, Z. Moser, R.E. Watson, M. Weinert, Journal of Phase Equilibria 17, 173 (1996).

[16] M. Ellner, K. Kolatschek, B. Predel, Journal of Less-Common Metals 19, 294 (1969).

[17] K. Schubert, "Kristallstrukturen zweikomponentiger Phasen", Springer-Verlag, Berlin (1964).

[18] V.J. Malkin, V.V. Pokidishev, Izvest. Akad. Nauk. SSSR, Metally 2, 166 (1966).

[19] N. Masahasi, H. Kawazoe, T. Takasugi, O. Izumi, Zeitschrift fuer Metallkunde 78, 788-794 (1987).

[20] C.C. Yia, K. Ishida, T. Nishizawa, Metallurgical and Materials Transactions A 25A, 473-485 (1994).

[21] Binary Alloy Phase Diagrams, 2nd ed., T.B. Massalski, ed. ASM INTERNATIONAL, Metals Park, OH, (1990).

[22] Y. Himuro, Y. Tanaka, N. Kamija, I. Ohnuma, R. Kainuma, K. Ishida, Intermetallics 12, 635-643 (2004).

[23] Y. Himuro, Y. Tanaka, I. Ohnuma, R. Kainuma, K. Ishida, Intermetallics 13, 620-630 (2005).

[24] A.J. Bradley, J. Iron Steel Institute 163, 19-30 (1949); 168, 233-244 (1951); 171, 41-47 (1952).